ICARUS **130,** 87–95 (1997)
ARTICLE NO. IS975799

The Mars Water Cycle: Determining the Role of Exchange with the Regolith

Bruce M. Jakosky

Laboratory for Atmospheric and Space Physics and Department of Geological Sciences, University of Colorado, Boulder, Colorado 80309-0392
E-mail: jakosky@argyre.colorado.edu

Aaron P. Zent

NASA/Ames Research Center, MS 245-3, Moffett Field, California 94035

and

Richard W. Zurek

Jet Propulsion Laboratory, MS 169-237, 4800 Oak Grove Dr., Pasadena, California 91125

Received October 18, 1996; revised June 27, 1997

The near-surface nighttime atmospheric water vapor concentrations inferred by Ryan *et al.* (J. A. Ryan, R. D. Sharman, and R. D. Lucich 1982. *J. Geophys. Res.* 87, 7279–7284) from Viking Lander air temperature measurements are a factor of 2–3 lower than the same quantities estimated from daytime atmospheric column water vapor abundances observed from the Viking Orbiters. We show that a physical model of the atmospheric boundary layer and regolith can produce a nighttime depletion of this magnitude by diffusion of water into the regolith and adsorption onto regolith grains. Quantitative validation of the model is not possible at present due to the lack of direct measurements of the near-surface atmospheric water vapor concentration and by uncertainties regarding surface regolith and atmospheric boundary layer properties. However, if the diurnal exchange of water vapor with the surface is as large as is suggested by the Viking Lander and Orbiter measurements, then the exchange of water between the atmosphere and regolith also is important in the seasonal cycle of water vapor. Further characterization of these processes can be made using measurements from the various landing site and atmospheric profiling experiments to be conducted by the Mars Pathfinder and Mars Surveyor Lander and Orbiter missions.

INTRODUCTION

The behavior of Mars atmospheric water vapor is important for understanding a variety of different aspects of the martian climate system. As one of the three major seasonal cycles of atmospheric constituents (the others being the dust and CO_2 cycles), the present distribution and annual cycling of water reflect both current and past climate processes. The behavior of atmospheric water vapor is physically linked to that of the other two cycles, and it can serve as an indicator of the state of the polar energy and mass balance. In particular, the long-term evolution of the polar deposits, and the cycles of deposition of mass into the polar regions and removal of it from them, is controlled in part by the integrated behavior of the seasonal water cycle acting over much longer time scales (see Jakosky and Haberle, 1992, for a synthesis of recent observations and models).

Previous analyses of the seasonal behavior of water have indicated the possible role of the polar caps in supplying water to the atmosphere (Jakosky and Farmer 1982, Haberle and Jakosky 1990) and of the atmospheric circulation in redistributing the water vapor (Barnes 1990, Houben *et al.* 1996). In addition, exchange of water between the atmosphere and the regolith is likely to occur on both a diurnal and seasonal basis (Fanale and Cannon 1971, 1974, Flasar and Goody 1976, Zent *et al.* 1993, Jakosky 1983a, b, Houben *et al.* 1997). The role of the regolith has only been inferred, however, based on its presumed adsorptive and diffusive properties (Jakosky 1983a, b) and on the ability of models of the seasonal atmospheric abundances of water vapor to better match the observed behavior when regolith exchange is included (Houben *et al.* 1997). A quantitative separation of the relative roles of the regolith and the retreating seasonal polar cap in supplying water to the atmosphere has been difficult, however, as they respond to the seasonal insolation forcing in a similar manner (Jakosky 1983b) and they both depend upon the vertical distribution of atmospheric vapor, which has not been directly measured.

0019-1035/97 $25.00

In particular, a key measurement required to assess the importance of water vapor exchange between atmosphere and regolith is the near-surface concentration of atmospheric water vapor. In the absence of direct measurement of this quantity, estimates have been made from the water vapor column abundances observed by the Mars Atmospheric Water Detectors (MAWD) on the Viking Orbiters (e.g., Jakosky 1983a) and from Viking Lander temperature measurements. Ryan *et al.* (1982) noted that the two approaches gave results which were comparable in magnitude, though not identical, and whose variations typically tracked one another.

Here, we reexamine the relationship between the nighttime near-surface water vapor concentration estimated from the Viking Lander observations and the (daytime) MAWD measurements of the total column of water. We confirm that there is a significant depletion during the night of near-surface atmospheric water vapor. Using a model of regolith–atmosphere exchange, we show that this inferred depletion is quantitatively consistent with the direct daily exchange of a significant amount of vapor between the atmosphere and the regolith. Our results also suggest a means of determining the role of the global regolith in the water cycle using measurements that can be carried out on future spacecraft missions.

COMPARISON OF VIKING ORBITER AND LANDER OBSERVATIONS

The Viking orbiters measured the integrated column abundance of water vapor in the atmosphere using the Mars Atmospheric Water Detection (MAWD) experiment (e.g., Farmer *et al.* 1977, Jakosky and Farmer 1982). Observations consisted of solar reflection measurements made at five closely spaced wavelengths in and between water vapor absorption lines. From the relative absorption of sunlight in the bands, the number of molecules of water vapor along the path traveled by the sunlight as it passed through the atmosphere could be determined. The uncertainty in the measurement is thought to be less than about 15%; however, the derived abundances may be biased toward low values during periods of high atmospheric dust opacity when the lower atmosphere may be obscured from view (Jakosky and Farmer 1982). Figures 1a and 2a show the seasonal cycle of water vapor as measured over the Viking Lander-1 and -2 sites, respectively. In each case, the symbols represent the daily averages of the atmospheric water column as measured by both orbiters in a box centered on the landing site and measuring 5° of latitude on a side. Because of the orbit and viewing geometry, each landing site was not observed every day.

The Viking landers did not have an instrument designed to detect atmospheric water vapor. However, during the night, the observed rate of decline of the atmospheric temperature at the 1.6-m height of the meteorology boom decreased for a period of about an hour and then resumed its original value (see Fig. 3). This inflection occurred every night at both landing sites, except when obscured by the thermal plume of the Lander itself or when there were known instrumental artifacts or data dropouts (Ryan *et al.* 1982). Based on the behavior of this inflection and the detection of enhanced atmospheric opacity at night (Pollack *et al.* 1977), Ryan and Sharman (1981) interpreted the nighttime temperature inflection to be a radiative effect due to the formation of an ice fog and thus the result of atmospheric saturation and condensation of water vapor. Their model of potential radiative effects of such an ice fog produced effects comparable in magnitude to the observed temperature deviation, although details of the variation with time were not well reproduced. Ryan *et al.* (1982) compared the surface water vapor concentration (and the mass mixing ratio) with the Viking MAWD column abundances and noted that they tracked each other seasonally at the two Viking Landing sites except possibly during dust storms and during northern autumn and winter at the higher-latitude VL-2. Ryan and Sharman (1981) had previously noted the possibility of a nighttime deficit of water vapor, but did not pursue this possibility.

The temperature at which the frost point was reached is a unique indicator of the water vapor molecular number density, through the saturation vapor pressure function and the ideal gas law. If water vapor exponentially decreases with a constant scale height H_w, then the surface vapor density D_w and the column abundance W_c are related as

$$W_c = H_w * D_w. \quad (1)$$

If water vapor is uniformly mixed with height, then $H_w = H$, the atmospheric scale height. For ease of comparison with the MAWD water vapor measurements, we have multiplied the number densities derived by Ryan *et al.* (1982) by a nominal atmospheric scale height of 10 km; these numbers are displayed in Figs. 1a and 2a. (Ryan *et al.*, 1982, compared logarithmic curves of W_c and D_w, examining the relatively constant offset.)

Although there are very few days when orbiter and lander measurements allow a direct comparison, a general offset between the two can be seen. Figures 1b and 2b show the ratio of the lander to the orbiter abundances, binned in increments of 30° of L_s to facilitate comparison. At the VL-1 site, the lander abundance is about 0.4–0.6 times the orbiter abundance. The variation seen at an L_s of about 270° appears to be due primarily to the vagaries of binning sparse data (see Figs. 1a and 2a). At the VL-2 site, the ratio is about 0.4 for most of the spring and summer seasons. During the winter, the lander-derived abundances drop precipitously, presumably due to the very cold near-

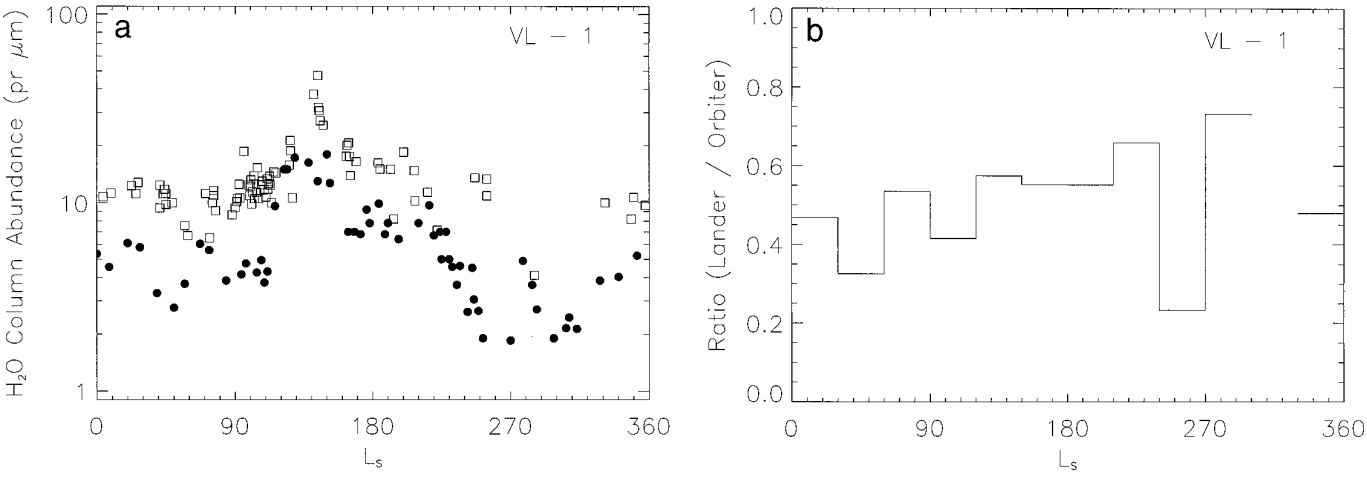

FIG. 1. (a) Measurements of the atmospheric water vapor abundance at the VL-1 site. Open boxes are orbiter MAWD measurements of the column abundance, shown as daily averages of values with a 5° box centered on the landing site. Closed circles are the surface number density inferred from the atmospheric temperature nighttime inflections, multiplied by the nominal atmospheric scale height of 10 km for comparison with orbiter measurements. (b) Ratio of the orbiter-derived abundance to the lander-derived abundance, averaged over 30° of L_s.

surface atmosphere near the periphery of the seasonal CO_2 polar cap. This drop was discussed in detail by Ryan *et al.* (1982). Our emphasis here is on the general reduction of 40–60% when compared with the orbiter-derived abundances.

The uncertainties in both the lander and orbiter measurements are small enough that it is unlikely that a ratio of 0.5 can result from measurement error. The MAWD orbiter measurements are accurate to perhaps 15% (Farmer *et al.* 1977, Jakosky and Farmer 1982). If there is dust obscuring the water vapor from view, the actual water columns would be larger than indicated by MAWD, further accentuating the discrepancy. Use of an incorrect scale height in the calculations would not introduce a factor of 2 uncertainty into estimates of the surface concentration, as the water vapor should be mixed throughout the planetary boundary layer and above by convective overturning during the day. If water vapor were to be distributed with a scale height smaller than that of the bulk atmosphere, then, again, the discrepancy would be further accentuated.

The VL-1 temperature measurements are good to better than 1 K, corresponding also to about a 15% uncertainty in the water vapor number densities. At VL-2, the primary temperature detector was inoperative, and the uncertainty in the secondary measurement is about 3 K, resulting in an uncertainty of less than 50%. At both sites, the major

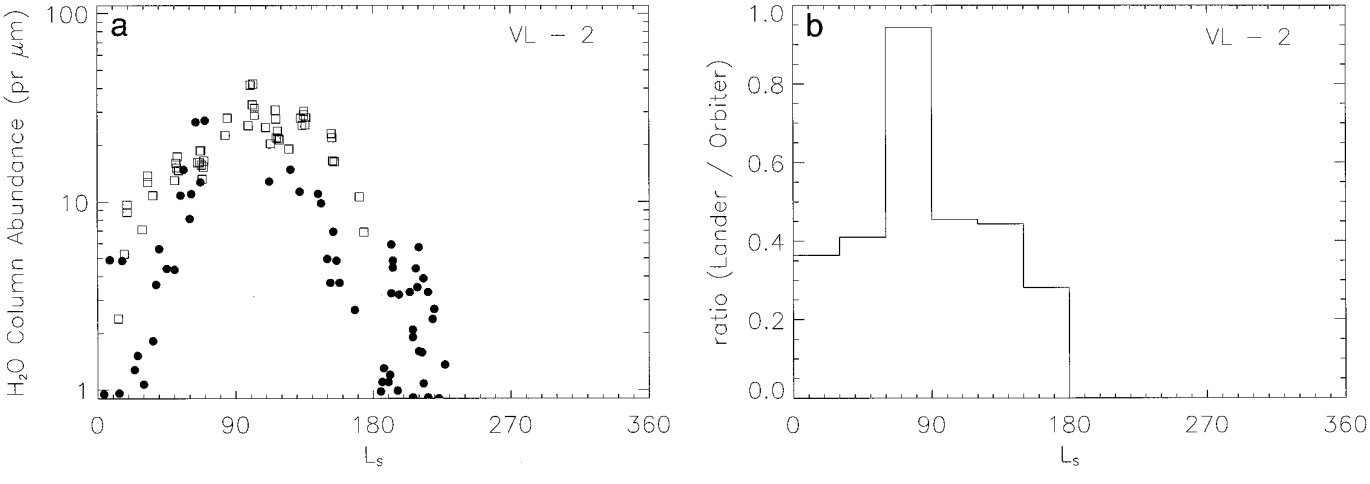

FIG. 2. (a) Measurements of the atmospheric water vapor abundance at the VL-2 site. Symbols are the same as in Fig. 1. (b) Ratio of the orbiter-derived abundance to the lander-derived abundance, averaged over 30° of L_s.

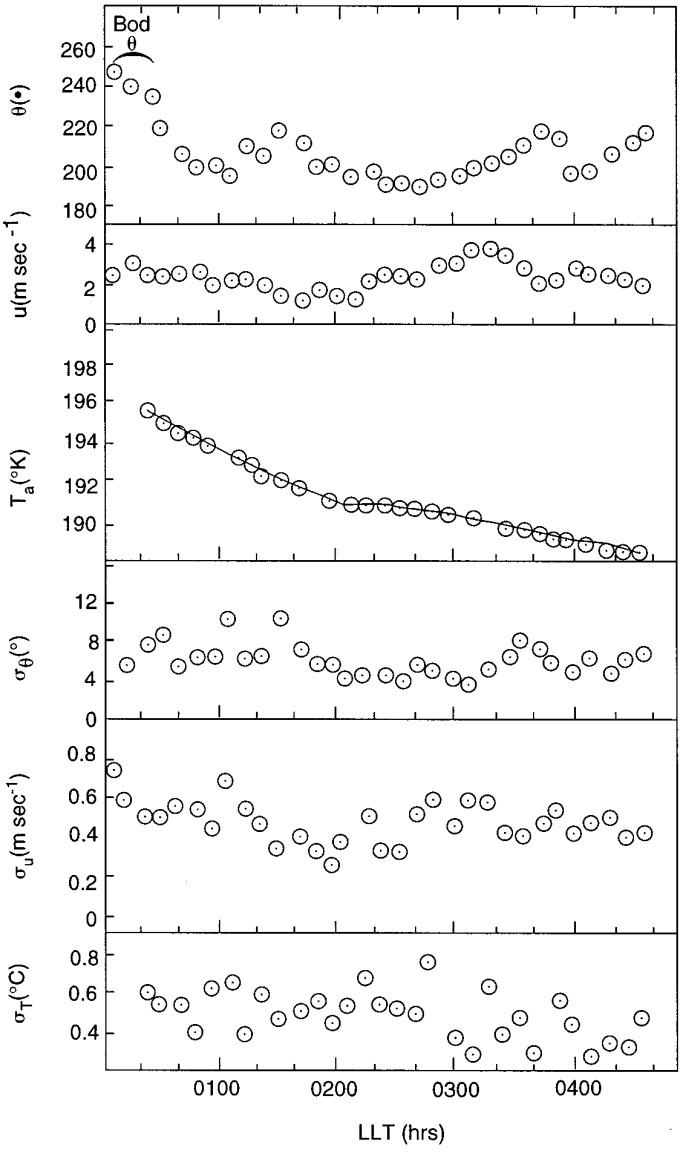

FIG. 3. Example of inflection in the nighttime atmospheric temperatures as measured at the VL-1 site. Additional meteorology parameters also are shown; from top, they are wind direction, wind speed, atmospheric temperature, and the standard deviations of the three parameters. Each is shown as a function of local time of day, referenced to local midnight, for VL-1 sol 21. (From Ryan *et al.* 1982.)

uncertainty may be the interpretation of the inflection point as being due to reaching the local frost point. However, as noted above, the pervasiveness and character of the signal argue convincingly that it does reflect the saturation state of the near-surface atmosphere (Ryan and Sharman 1981). One possibility for the nighttime depletion is the formation of the ice fog which is presumed to produce the inflection in the Lander temperature measurements. Less than 1 precipitable micrometer equivalent of ice fog can have the required radiative effect (Ryan and Sharman 1981), and that would most likely be distributed over at least several hundred meters. It is unlikely, though, that the presence of a fog would account for the factor of 2 reduction in near-surface water vapor concentrations from the daytime values. If the inflection is due to reaching the saturation point, then fogs would form after this time; there would be no fog present initially. That is, the nighttime depletion occurs prior to saturation.

In summary, the lander-derived nighttime abundances are lower than the daytime MAWD-derived abundances, indicating that there is a nighttime depletion of atmospheric water vapor near the surface. The most plausible physical mechanism that might explain this behavior both quantitatively and qualitatively throughout the year is the nighttime depletion of the lower atmospheric water vapor by the adsorption of water vapor onto regolith grains as the regolith cools, and the subsequent diffusion of water into the regolith. Models of the nighttime depletion of the lower atmosphere expected for reasonable physical assumptions regarding the regolith are discussed in the next section.

BOUNDARY-LAYER/REGOLITH EXCHANGE

We use a model of the atmospheric boundary layer and the upper portion of the regolith to demonstrate the role of the regolith in the diurnal cycling of water vapor and the depletion of the lower part of the atmosphere. The boundary layer model used in this paper is a derivative of the model described by Zent *et al.* (1993) and can be considered to be an updated version of the model originally developed by Flaser and Goody (1976). It has been amended to include the results of more recent H_2O adsorption measurements and further altered so that the user can specify the final atmospheric H_2O column to which the model should converge. The model description below is based on Zent *et al.* (1993), to which the reader is referred for a more complete discussion.

The atmospheric portion of the boundary layer model is taken from Haberle *et al.* (1993). The model solves a momentum and energy equation in which the dependent variables are assumed to be functions of height and time. The momentum equation includes terms for the pressure gradient, Coriolis, and friction forces; the energy equation includes terms for radiation and turbulence. They are solved on a vertical grid with 85 nonuniformly spaced layers which extend from the surface to 40 km altitude. The pressure gradient term is calculated by assuming that the winds are driven by buoyancy-driven slope flow. Radiative heating is calculated assuming that the martian dust and CO_2 are the only active components and that the dust is uniformly mixed. The frictional forces and turbulent heating are parameterized in terms of a diffusion process. The eddy coefficients are calculated based on the formalism of

Mellor and Yamada (1982) and are functions of the local Richardson number and a mixing length. The mixing length is a function of height; it is small near the surface and approaches a maximum value asymptotically as z goes to infinity. We assume that H_2O is transported as a passive tracer. The model allows for changes in the H_2O mixing ratio due to convergence in the vertical flux of moisture by turbulence. At the base of the atmosphere, the flux is partially determined by the H_2O adsorption isotherm, which is assumed to control the partial pressure and, hence, the mixing ratio. The moisture flux at the surface is communicated to the regolith by requiring conservation of mass in the column. Thus, the flux of water entering the regolith is always equal to the flux leaving the atmosphere.

The subsurface thermal model solves the heat conduction equation, assuming energy balance at the surface. Both the thermal and H_2O transport equations are solved on a 15-point exponential grid, which extends from the surface to 8.3 m depth. The deepest grid point is set below the penetration depth of the annual thermal wave to simplify treatment of the lower boundary condition; further details are in Zent *et al.* (1993). The transport model, which moves H_2O vertically through the regolith, assumes that all transport is via diffusion, which takes place according to Fick's law. We assume that all H_2O molecules must be in either vapor, adsorbed, or ice phases. In this work, we make a new assumption regarding the form of the adsorption isotherm. That is, we assume that the adsorption α of water onto the surfaces of the regolith materials as a function of temperature T and the number density γ of H_2O molecules in the pore space goes as

$$\alpha(\gamma, T) = \rho_s A_s M_i \left(\frac{K^*P}{1 + K^*P}\right)^{\nu}, \qquad (2)$$

where ρ_s is the density of the regolith material in kg m^{-3}, A_s is the specific surface area of the regolith material, assumed for this purpose to be 10^5 m^2 kg^{-1}, and M_i is the mass of 1 m^2 of adsorbed H_2O molecules (2.84×10^{-7} kg monolayer^{-1}). The adsorption α is in units of kg/m^3. The term in parentheses is the Guggenheim isotherm. Zent and Quinn (1995) measured adsorption of H_2O onto palagonite under Mars-like conditions, and Zent and Quinn (1997) have recently compared the data to several forms of adsorption isotherm which account for heterogeneity of the adsorption sites. They found that the palagonite data is best fit by an expression such as this, and derived the following parameters by least-squares fitting

$$K_0 = 1.57 \times 10^{-8}, \quad e = 2573.9, \quad \nu = 0.48, \qquad (3)$$

where

$$K^* = K_o \exp(e/T) \qquad (4)$$

$$P = \gamma k T / m_w. \qquad (5)$$

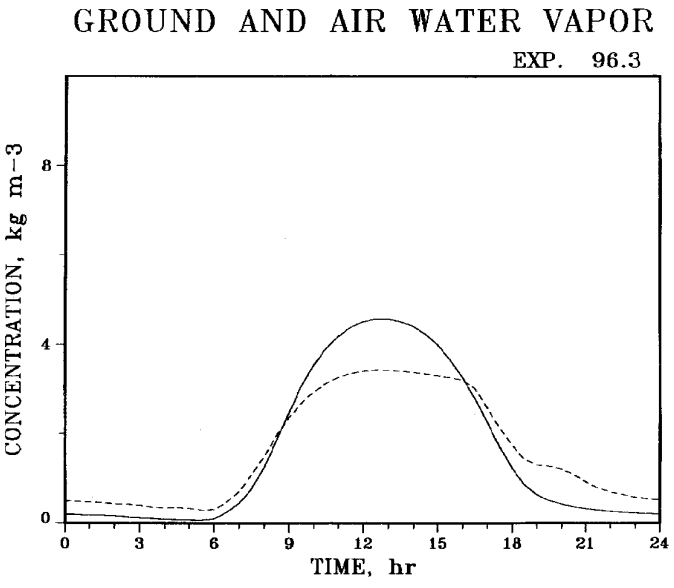

FIG. 4. Diurnal variation of the water vapor number density at the surface (solid line) and at 1.6 m altitude (dashed line) as predicted by the boundary-layer/regolith model for the VL-1 site, at an L_s of 110°.

The last equation is equivalent to assuming that H_2O in the pores obeys the ideal gas equation, with m_w being the mass of a water molecule. The diffusion coefficient in Fick's Law is then scaled by the derivative of Eq. (2) with respect to γ, $d\alpha/d\gamma$. The numerical procedure was to assume that the atmosphere is initially dehydrated and that the regolith is charged with an equilibrium amount of water, equivalent to approximately 1.5 kg m^{-3} of regolith. For each simulation, the model is given the season (L_s), the total atmospheric pressure (from the Viking Lander measurements), and a target atmospheric H_2O column, which is chosen to match the MAWD observations at the same season. The model is run, and at the end of each complete sol the total column is summed. If the atmospheric column is greater than 105% of the target value, the amount of H_2O in each vertical layer in both the atmosphere and regolith is scaled downward by the ratio of (target/column). Only after the model has run for three consecutive sols and yielded atmospheric columns within 5% of the target does the model declare equilibrium and report the results. The goal of this procedure is to model the water cycle that would be in equilibrium with the atmospheric column actually observed by Viking at that season. For the final sol, the model also reports the frost-point temperature of the atmosphere at the 1.6-m grid point at the time that saturation is reached. This is the datum equivalent to the frost-point measurements reported by Ryan *et al.* (1982).

Figure 4 shows the diurnal variation of the water vapor number density at 1.6-m height above the surface, as predicted by this model. Notice that the nighttime number

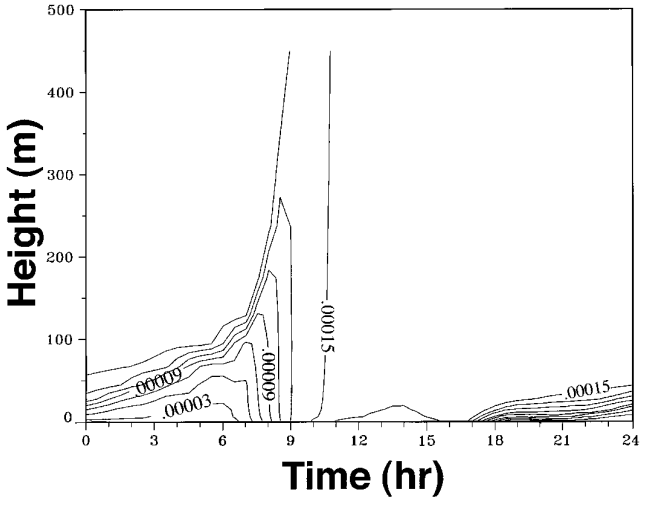

FIG. 5. Water vapor mixing ratio contoured as a function of altitude and local time of day, as predicted by the boundary-layer/regolith model for the VL-1 site with the same model as shown in Fig. 4.

density is reduced substantially from the daytime value. In the model, this is a direct result of the adsorption of water vapor on the regolith grains as the regolith cools off, followed by diffusion of water vapor from the atmosphere into the regolith that results from the newly created gradient in the number density. As much as 90% of the water in the bottom several hundred meters of atmosphere is removed by this mechanism (Fig. 5). During the following day, the regolith heats up again, desorbs its water vapor, and the water diffuses back into the atmosphere. The high rate of mixing during the day that results from the dynamical instability of the lower atmosphere ensures that the daytime mixing ratio of water vapor will be constant with altitude throughout the boundary layer.

The seasonal variation in the size of this depletion is shown in Fig. 6 for the VL-1 site. The model was run at specific seasons, using the appropriate subsurface temperatures and atmospheric temperature and water vapor boundary conditions. The nighttime depletion occurs regularly throughout the year. The VL-2 site showed a similar pattern of nighttime depletion throughout the year, although there are some additional complications that result from wintertime surface temperatures that are substantially lower than the atmospheric temperatures.

Notice that the magnitude of the nighttime depletion predicted by the boundary layer model is comparable to that which is observed. This depletion factor can be affected by a number of processes, such that the close agreement may be fortuitous. Processes that can affect the nighttime depletion include: (i) Uncertainties in the frost-point temperatures and saturation vapor pressures inferred from the Viking Lander temperature data. (ii) Adsorption properties of the regolith that are different from those assumed in the model. Either a less- or a more-adsorbing regolith will affect the ability to draw water from the atmosphere. (iii) Diffusive properties of the regolith that are different from those assumed in the model. In particular, the presence of a duricrust, as was seen at the Viking landing sites (Moore and Jakosky 1989) and which may be present globally (Jakosky and Christensen 1986), may inhibit diffusion, and the degree of crust formation will affect the ability of water to exchange. (iv) A vertical distribution of atmospheric water vapor that differs from uniform mixing. Changing the water vapor scale height will change the near-surface number density (and hence affect the nighttime depletion) without changing the total amount of atmospheric water. (v) Uncertainties connected to the nighttime vertical mixing of the atmosphere, which is not well understood. The degree of mixing will affect the vertical extent and therefore the magnitude of nighttime depletion. Although these several effects may change the magnitude of the depletion of atmospheric water vapor, it is unlikely that they could introduce an apparent depletion so consistently if there was none present to begin with.

As a result, it is clear that the discrepancy seen between the Viking Lander and Orbiter measures of water vapor can result from the nighttime depletion of atmospheric

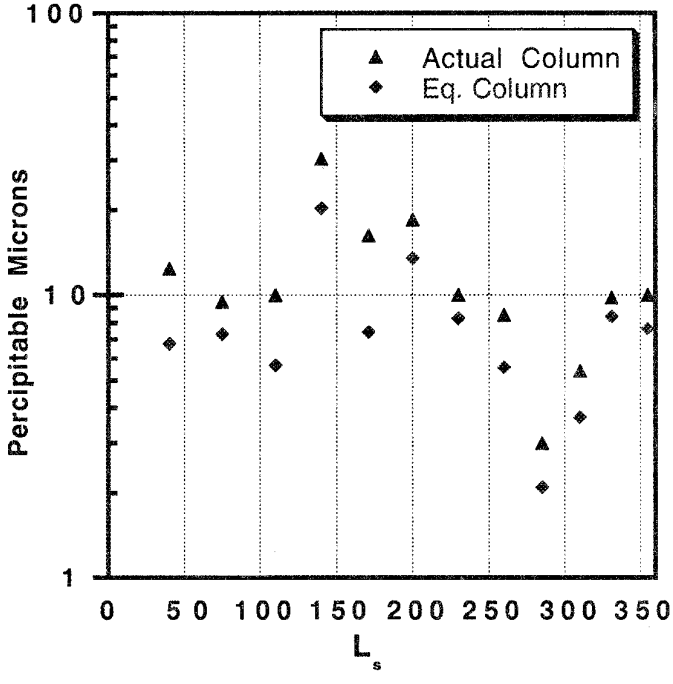

FIG. 6. Comparison of observed water vapor column abundances at the VL-1 site with model predictions. This figure is analogous to Fig. 1a and shows the equivalent column abundance calculated from the near-surface number density at the time of nighttime saturation (diamonds). The actual column in the model was taken to be the same as the observed value at each season (triangles).

water vapor by diffusion into the regolith. Both the observations alone and the boundary-layer model results support this conclusion. Unfortunately, however, the uncertainties in the vertical distribution of water vapor within the atmosphere and in the daytime near-surface number density preclude a unique determination of the actual amount of water that exchanges diurnally.

DETERMINING THE ROLE OF THE REGOLITH IN THE WATER CYCLE

The present analysis immediately points out the need for surface and atmospheric boundary layer measurements in order to quantify the role of exchange with the regolith in the seasonal water cycle. Unlike atmospheric transport of water, which is determined by the global distribution of atmospheric water vapor and the global pattern of winds at all altitudes, the exchange of water with the regolith is a local phenomenon. It depends only on the water vapor number density in the atmosphere at the surface and on the local diffusive and adsorptive properties of the regolith. Because the regolith properties are expected to vary spatially (for instance, possibly as the thermal inertia or degree of duricrust formation varies spatially; see Palluconi and Kieffer, 1981, and Christensen and Moore, 1992), a number of landers would be required in order to map out the spatial variation of the regolith response. At each site, the diurnal variation seen in the atmospheric water vapor density would be used to determine the local role of exchange with the regolith. Combined with measurements throughout the entire vertical column, these surface data could provide quantitative validation of physical models of the water vapor exchange and a direct estimate of the amount of water that exchanges. These results would be combined with global atmospheric measurements pertinent to the water vapor transport and polar measurements of seasonal supply and loss of water from the caps and would result in an understanding of all the aspects of the seasonal water cycle.

A wide variety of measurements to be made on upcoming and planned missions will address these issues directly. The Mars Pathfinder (MP), Mars Global Surveyor (MGS), and the Mars Surveyor Program (MSP) 1998 Orbiter and Lander (which also carries two short-lived penetrator micro-probes) will make several key measurements that address the exchange of water vapor between the atmosphere and surface directly.

Measurements to be made at the surface in 1997 by Mars Pathfinder (at a latitude of 19°) and in 1999 by the MSP '98 Lander (near −75°) include nighttime measurements of near-surface air temperatures, although power restrictions may limit the measurement frequency and seasonal duration as compared to Viking. Nearly identical imagers on

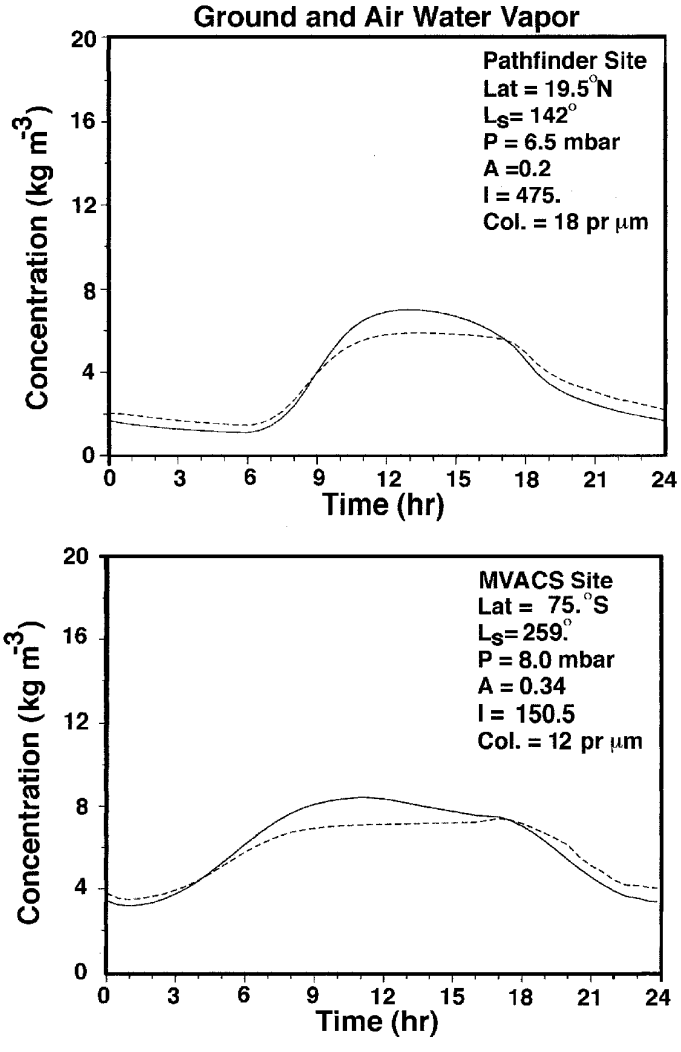

FIG. 7. Diurnal variation of the water vapor number density at the surface (solid line) and at 1.6 m altitude (dashed line), as predicted by the boundary-layer/regolith model (a) for the Mars Pathfinder landing site (latitude of 19°) at the time of the landing (L_s = 145°) and (b) for the Mars Surveyor 1998 Lander (−77°) after its projected arrival (L_s = 270°).

the two landers (Imager for Mars Pathfinder, IMP, on MP and Solid State Imager, SSI, on MSP '98) provide an advantage over Viking, in that water vapor column abundances may be measured from the lander itself by using broadband filters to view the differential spectral absorption of sunlight passing through the atmosphere. Thus, daylight observations are possible at the same site and during the same period that the nighttime inflection points are recorded.

Because of its high latitude and operation near summer solstice, the MSP '98 SSI will attempt to measure column abundances throughout most of a diurnal cycle. Our model calculations (Fig. 7) indicate that there is still enough diur-

nal forcing to produce a significant exchange of water vapor between atmosphere and surface, even at this high southern latitude. Comparison of results from the MP and MSP '98 Landers will provide key tests of models, given the different diurnal forcing at their respective latitudes and an anticipated large contrast in the thermal inertias of the two landing sites.

Regional and global contexts for the landed measurements will be provided by the MGS Thermal Emission Spectrometer (TES; Christensen *et al.* 1992) and the MSP '98 Pressure Modulator IR Radiometer (PMIRR; McCleese *et al.* 1992). TES measurements of surface temperatures will provide global fields of thermal inertia and surface albedo at much higher spatial resolution than current values based on Viking data. Furthermore, profiles of atmospheric temperature, dust, and ice extinction will be derived first from TES data (1997–1999) and then, with greater vertical resolution, from PMIRR measurements (1999–2001). Most importantly for the hydrological cycle, PMIRR is also designed to retrieve vertical profiles of atmospheric water vapor, which provide a direct characterization of its scale height and how it changes with season and location (McCleese *et al.* 1992). However, neither of these passive atmospheric sounders will resolve the planetary boundary layer, even though PMIRR profiles should extend to within 4 km of the surface.

With regard to validating the present model of water vapor exchange between the atmosphere and surface, the measurements discussed above are relatively indirect. The best test of the model predictions is likely to come from the MSP '98 Lander's integrated Mars Volatiles and Climate Surveyor (MVACS) package. MVACS, which includes the SSI described earlier, will use a tunable diode laser to make high-spectral-resolution measurements of the absorption of light by near-surface atmospheric water vapor during the full diurnal cycle. This measured diurnal variation of near-surface vapor, and its change as the south polar summer wanes, describes both the forcing and response function. This will short-circuit the model's treatment of the planetary boundary layer and provide hard constraints on the modeling of the subsurface processes. Conversely, comparison of the measured near-surface water vapor concentration with estimates derived from the MVACS sun views (i.e., column abundances from SSI), temperature sensors (i.e., nighttime inflection points), and the PMIRR extrapolated profiles of atmospheric vapor will test models of boundary layer processes. If the models show consistent relationships between these, then the TES surface data and PMIRR vapor measurements will enable global estimates of the relative contributions of the regolith to the martian seasonal water cycle. Based on the present modeling of Viking data, we expect that contribution to be significant.

ACKNOWLEDGMENTS

We thank Linda Sauter for compiling the data for Figs. 1 and 2 and James Murphy for valuable discussions. We appreciate comments from Fraser Fanale and from an anonymous reviewer. This research was supported in part by the NASA Planetary Atmospheres Program, through Grant NAGW-771 at the University of Colorado, RTOP 151-01-60-11 at NASA/Ames Research Center, and carried out in part at the Jet Propulsion Laboratory, California Institute of Technology.

REFERENCES

Barnes, J. R. 1990. Transport of dust to high northern latitudes in a martian polar warming. *J. Geophys. Res.* **95,** 1381–1400.

Christensen, P. R., and H. J. Moore 1992. The martian surface layer. In *Mars* (H. Kieffer, B. Jakosky, C. Snyder, and M. Matthews, Eds.), pp. 686–729. Univ. of Arizona Press, Tucson.

Christensen, P. R., D. L. Anderson, S. C. Chase, R. N. Clark, H. H. Kieffer, M. C. Malin, J. C. Pearl, J. Carpenter, N. Bandiera, F. G. Brown, and S. Silverman 1992. Thermal emission spectrometer experiment: The Mars Observer Mission, *J. Geophys. Res.* **97,** 7719–7734.

Clancy, R. T., A. W. Grossman, M. J. Wolff, P. B. James, D. J. Rudy, Y. N. Billawala, B. J. Sandor, S. W. Lee, and D. O. Muhleman 1996. Water vapor saturation at low altitudes around Mars aphelion: A key to Mars climate? *Icarus* **122,** 36–62.

Fanale, F. P., and W. A. Cannon 1971. Adsorption on the martian regolith. *Nature* **230,** 502–504.

Fanale, F. P., and W. A. Cannon 1974. Exchange of absorbed H_2O and CO_2 between the regolith and atmosphere of Mars caused by changes in surface insolation. *J. Geophys. Res.* **79,** 3397–3402.

Farmer, C. B., D. W. Davies, A. L. Holland, D. D. LaPorte, and P. E. Doms 1977. Mars: Water vapor observations from the Viking orbiters. *J. Geophys. Res.* **82,** 4225–4248.

Flasar, F. M., and R. M. Goody 1976. Diurnal behavior of water on Mars. *Planet. Space Sci.* **24,** 161–181.

Haberle, R. M., and B. M. Jakosky 1990. Sublimation and transport of water from the north residual polar cap on Mars. *J. Geophys. Res.* **95,** 1423–1437.

Haberle, R. M., H. C. Houben, R. Hertenstein, and T. Herdtle 1993. A boundary-layer model for Mars: Comparison with Viking Lander and entry data. *J. Atmo. Sci.* **50,** 1544–1559.

Hart, H. M. 1989. *Seasonal Changes in the Abundance and Vertical Distribution of Water Vapor in the Atmosphere of Mars.* Ph.D. dissertation, U. Colorado, Boulder.

Houben, H., R. M. Haberle, R. E. Young, and A. P. Zent 1997. Modeling the martian seasonal water cycle. *J. Geophys. Res.* **102,** 9069–9083.

Jakosky, B. M. 1983a. The role of seasonal reservoirs in the Mars water cycle. I. Seasonal exchange of water with the regolith. *Icarus* **55,** 1–18.

Jakosky, B. M. 1983b. The role of seasonal reservoirs in the Mars water cycle. II. Coupled models of the regolith, the polar caps, and atmospheric transport. *Icarus* **55,** 19–39.

Jakosky, B. M., and P. R. Christensen 1986. Are the Viking lander sites representative of the surface of Mars? *Icarus* **66,** 125–133.

Jakosky, B. M., and C. B. Farmer 1982. The seasonal and global behavior of water vapor in the Mars atmosphere: Complete global results of the Viking atmospheric water detector experiment. *J. Geophys. Res.* **87,** 2999–3019.

Jakosky, B. M. and R. M. Haberle 1992. The seasonal behavior of water

on Mars. In *Mars* (H. Kieffer, B. Jakosky, C. Snyder, and M. Matthews, Eds.), pp. 969–1016. Univ. of Arizona Press, Tucson.

McCleese, D. J., R. D. Haskins, J. T. Schofield, R. W. Zurek, C. B. Leovy, D. A. Paige, and F. W. Taylor 1992. Atmospheric and climate studies using the Mars Observer Pressure Modulator Infrared Radiometer. *J. Geophys. Res.* **97,** 7735–7757.

Mellor, G. L., and T. Yamada 1982. Development of a turbulence closure model for geophysical fluid problems. *Rev. Geophys.* **20,** 851–875.

Moore, H. J., and B. M. Jakosky 1989. Viking landing sites, remote sensing observations, and physical properties of martian surface materials. *Icarus* **81,** 164–184.

Palluconi, F. D., and H. H. Kieffer 1981. Thermal inertia mapping of Mars from 60S to 60N. *Icarus* **45,** 415–426.

Ryan, J. A., and R. D. Sharman 1981. H_2O frost point detection on Mars? *J. Geophys. Res.* **86,** 503–511.

Ryan, J. A., R. D. Sharman, and R. D. Lucich 1982. Mars water vapor, near-surface. *J. Geophys. Res.* **87,** 7279–7284.

Zent, A. P., and R. C. Quinn 1995. Simultaneous adsorption of CO_2 and H_2O under Mars-like conditions and application to the evolution of the martian climate. *J. Geophys. Res.* **100,** 5341–5349.

Zent, A. P., and R. C. Quinn 1997. Measurement of H_2O absorption at Mars-like conditions: Effects of adsorbent heterogeneity. *J. Geophys. Res.* **102,** 9085–9095.

Zent, A. P., R. M. Haberle, H. C. Houben, and B. M. Jakosky 1993. A coupled subsurface-boundary layer model of water on Mars. *J. Geophys. Res.* **98,** 3319–3337.